COBEM 2023 27TH INTERNATIONAL CONGRESS OF MECHANICAL ENGENEERING

ABCM Brazilian Society of Mechanical Sciences and Engineering
27th ABCM International Congress of Mechanical Engineering
December 04-08, 2023, Florianópolis-SC, Brazil

# COB-2023-0299
# PRESSURE DROP ANALYSIS IN EMULSIONS FLOW

**Ligia Gaigher Franco**
**Murilo Zucatelli Elias**
**Rayane Reinholz Boone Corona**
**Edimilson Kempin Júnior**
**Juliana Thomes Alves Roberti**
**Rogerio Ramos**
Universidade Federal do Espírito Santo - UFES
Av. Fernando Ferrari, 514, Campos Universitário Goiabeiras, Vitória ES, CEP 29075-910, Brazil.
ligiagaigherf@gmail.com, murilozucatelli@gmail.com, rayane.boone@gmail.com, edimilsonkj@gmail.com, juliana_thomes@hotmail.com, rogerio.ramos@ufes.br

**Renato do Nascimento Siqueira**
Intituto Federal do Espírito Santo (Campus São Mateus)
renatons.ifes@gmail.com

***Abstract:*** *This paper presents an analysis of pressure drop in water-in-oil emulsion flows, with water volume fraction from 7% to 25%. Empirical correlations are evaluated to estimate density and viscosity. The pressure gradient is estimated assuming homogeneous flow model. The predicted values are compared against experimental data. Results indicate that the density model exhibits errors of less than 1.5%, demonstrating its accuracy. The best viscosity model presents errors between 3% and 16%. The estimated pressure gradient underpredicts the pressure loss, with deviations ranging from -5% to -28%. These findings indicate the challenges associated with accurately predicting pressure drop in emulsion flow and highlight the need for further investigation of existing models.*

***Keywords:*** *emulsion, pressure drop, water-in-oil emulsions, multiphase flow*

## 1. INTRODUCTION

Emulsions are heterogeneous mixtures of two or more immiscible liquids in a dispersed system. In the presence of an emulsifying agent and mechanical perturbation, this mixture behaves as a homogeneous system. Emulsions occur in various industrial sectors, such as food, pharmaceutical, and petrochemical. Focusing on the application of oil production in deep water, stable emulsions form during oil extraction, from the reservoir to the choke valve, in the interaction between saline water and crude oil (Alsabagh et al., 2016).

Although the interfacial mechanisms resulting in emulsion drop breakdown and/or coalescence are not yet fully understood, it is known that the shear breaks the emulsion droplets, acting to convert a droplet into tiny and stable droplet sizes (van der Zande, 1998). The process of separating water-in-oil emulsions with small droplet sizes employs large amounts of demulsifiers (Sullivan et al., 2008), which is undesirable because of theirs high costs as well as oxidation of facilities and tanks.

In this context, the Emulsion Flow Circuit located at NEMOG lab/UFES aims to conduct laboratory-scale studies about the impact of pipe fittings (e.g., pumps, knees and valves) on the droplet size distribution (DSD) of water-in-oil emulsions. The flowing fluids are stable emulsions which mimic the behavior of water-in-oil emulsion from Brazilian pre-salt reservoirs. It is composed of saline water, mineral oil and surfactants. The flow circuit used in this work presents flow similarity with an actual pre-salt oil extraction plant by equality of Weber number (Kempin Júnior et al., 2022). Besides, the emulsions present transport properties and chemical profile similar to a reference crude oil, considering the physical-chemical evaluation and infrared absorption spectrometry (Corona et al., 2023).

An important aspect for the sizing of pumps, compressors and instrumentation is the pressure drop estimation. For single-phase flows, pressure drop prediction is well established and consolidated. However, in multiphase flows, such as emulsion flow, pressure drop modeling is still a technological challenge due to the lack of experimental data available.

Pressure gradient in dispersed liquid-liquid flow was studied by Angeli et al. (1999) and Guet et al. (2006). In both studies, the ratios of oil viscosity and water viscosity are less than 10. For emulsion flow studies, it is reasonable to use a homogeneous no-slip model to compute the frictional pressure gradient. The mixture is therefore considered as a single fluid with an equivalent mixture density and an effective viscosity. For the friction factor, the same model used in single phase flows is employed (Guet et al., 2006). Rodriguez et al. (2006) showed that homogeneous no slip model described reasonably the pressure drop of oil-water dispersions.

From this perspective, the aim of this work is to analyse the pressure drop imposed by water-in-oil emulsion flows, with viscosity ratio of 130 and water volume fraction from 7% to 25%. The analysis is performed in a horizontal section with aspect ratio L/D = 415. Empirical correlations are evaluated for estimating mixture properties, such as density and viscosity. These models are compared with experimental data.

## 2. METHODOLOGY

### 2.1 Emulsion characterization

The working fluids are water-in-oil emulsions, composed of oil as continuous phase and saline water as dispersed phase. The water volumetric concentration ranges from 1% to 25%. The continuous phase is composed by mineral oil Mobil AW68 with 0.1% of the surfactant Triton X-114. The dispersed phase is comprised of deionized water with 35 g/L of NaCl. After the preparation of each phase, water and oil are mixed in batches of 50 L by mechanical agitation using the Ultra Turrax T65. Each experiment requires 400 L of emulsion. A key aspect for the produced emulsions is the high stability period for droplet size (more than 24 hours).

Prior to the experiments in the flow circuit, emulsions are characterized in aspects of interfacial tension, density, viscosity, water fraction and droplet size distribution.

Interfacial tension $\sigma$ between oil phase and saline aqueous phase is performed by a Tensiometer SEO (Phoenix model MT), that uses the pendant-drop method. In this work, interfacial tension is 0.0025 N/m at 25°C.

The emulsion density $\rho$ is measured by the digital analyzer Anton Paar DSA5000M. The analyzer is in accordance with ASTM D5002 (2005). In this work, emulsion density is characterized from 20°C to 36°C.

The rheology of emulsions is obtained by a HAAKE MARS 60 rheometer and double gap coaxial cylinder measurement system, in accordance with ASTM D4402 (2015). The flow curves are obtained at temperatures of 25°C and 35°C and at shear rates range from 1 to 3000 $s^{-1}$; totalizing 600 dynamic viscosity measurement for each sample. Table 1 presents the characterization of oil and water phases in aspects of density and viscosity.

Table 1. Characterization of oil phase and water phase

| Property | Oil phase | Water phase |
|---|---|---|
| Density $\rho[kg/m^3]$ at 20°C | 872.7 | 1022.4 |
| Viscosity $\mu[Pa.s]$ at 25°C | 0.1319 | 0.0010 |
| Viscosity $\mu[Pa.s]$ at 35°C | 0.0800 | 0.0008 |

For each dispersed phase volumetric concentration, the water fraction is measured by potentiometric titration using Karl Fisher reagent without pyridine in a Metrohm titrator (model 870 Titrando) with double platinum electrode in accordance with ASTM D4377 (2006).

The droplet size distribution (DSD) of emulsions is obtained by laser diffraction technology by a Betterziser analyzer model ST and isoparaffin as a dispersing medium.

### 2.2 Experimental description

The emulsion flow loop is located at the flow lab of Research Group for Oil and Gas Flow and Measurement (NEMOG, in Portuguese), at Universidade Federal of Espírito Santo (UFES). The piping and instrumentation diagram (P&ID) of the experimental apparatus is shown in

Figure 1.

A 500 L tank (TK-01) is used for emulsion storage, homogenization and sampling. It supplies emulsion to a 750 L pressure vessel (V-01) by gravity. With this procedure, one expects that the original DSD of the original emulsion will not be significantly altered.

The pressure vessel (V-01) is equipped with pressure sensor (PT-01, model Warme WTP 4010 ), temperature sensor (TT-01, model Zurich T.420.I.H), differential pressure sensor (PDT-01, model Yokogawa EJA110E) for level monitoring and a pressure control valve (PCV-1, globe valve model Samson 3241 ) for air supply, if required.

Flow is promoted by a helical pump (P-01, model Helibombas 2HT-32), driven by a 4 CV electric motor coupled to a variable speed drive (model WEG CFW500). Downstream to the pump, the tubes are stainless steel made, with internal diameter of 21 mm.

After the pump, there is pressure transmitter (PT-02, model Microsensor M20) and a hydraulic accumulator (HA-01, model Ciltech). The latter one is installed in order to attenuate pressure fluctuations due to the positive displacement pump. The mass flow rate and density are monitored by a Coriolis flowmeter (FIT-01, model Micromotion 2700).

The test section for droplet size distribution is located after the Coriolis flowmeter, starting at the first upward vertical tube section. This section represents a production well and has 2.7 meters long. At the bottom, there is a gauge pressure

sensor (PIT-01, model Yokogawa EJA530E). Next, a 9.7-meter-long horizontal section represents the flowline. The gauge pressure is monitored by 2 sensors located at the beginning and at the end of this section (PIT-02 and PIT-03, model Yokogawa EJA530E). The second upward vertical section represents the riser and has 3.0 meters long. At the end of this section, there is a gauge pressure sensor (PIT-04, model Yokogawa EJA530E).

At the end of the riser section, the fluid flows through a hose to the upper emulsion tank (TK-02), for temporary storage of the emulsion after the test.

Although not used in this work, three fluid extraction devices (EXT) are installed in strategic locations along the flow circuit in order to evaluate droplet size distribution close to pipe fittings.

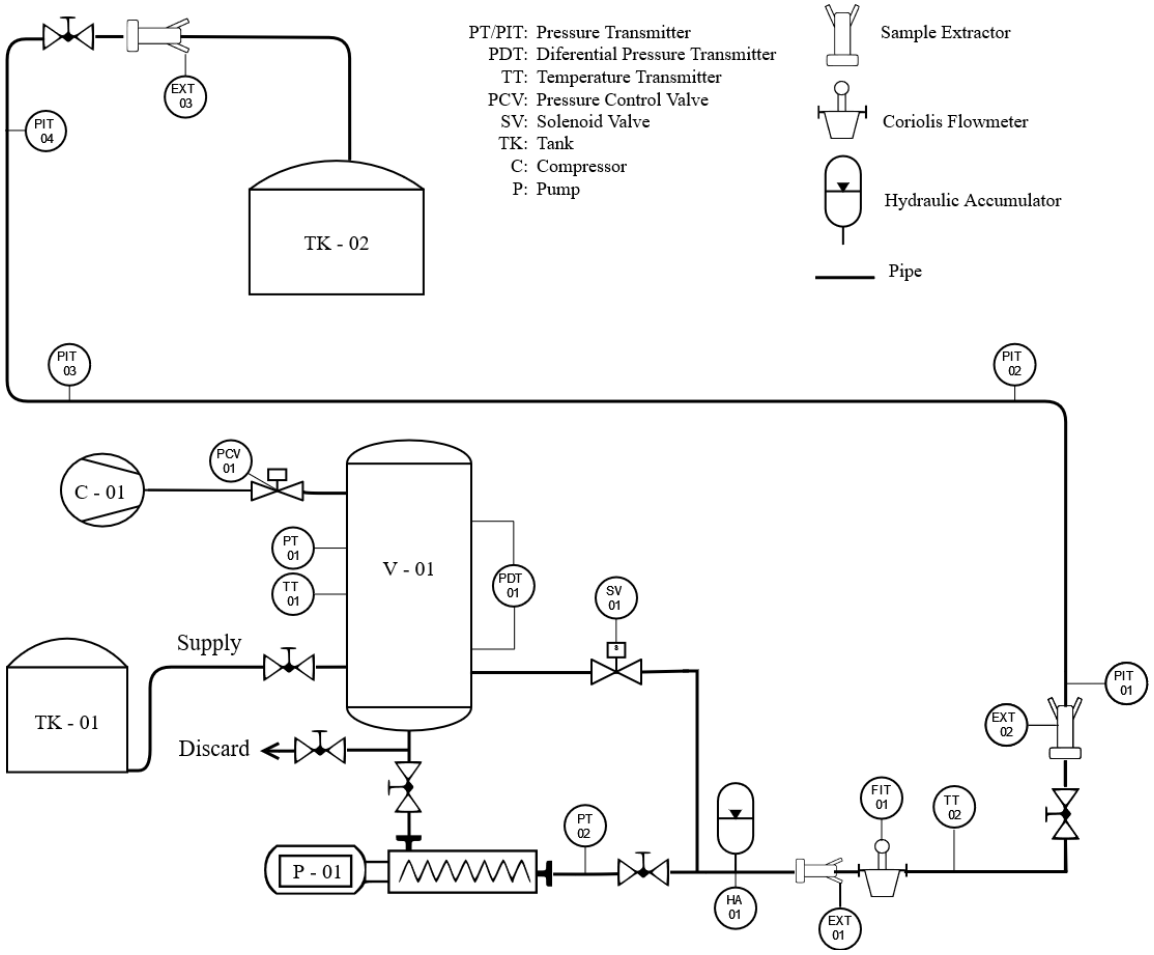


Figure 1. P&ID diagram of the system.

The pressure drop is evaluated in the horizontal section that represents the flowline. The distance between pressure taps PIT-2 and PIT-3 is 9.1 meters.

The experiment control and data acquisition system are integrated in a supervisory system based in the LabView platform.

### 2.3 Pressure gradient prediction

According to Wallis (2020), for homogeneous flow in equilibrium, as the one of stable emulsions, suitable average properties are determined and the mixture is treated as a pseudo fluid that obeys the usual equations for single-component flow. The required average properties are velocity, thermodynamic properties (temperature and density), and transport properties (viscosity). Hence, pressure drop can be predicted in a simplified way with good accuracy.

The homogeneous flow assumption requires that fluids must present: i) same velocity, ii) same temperature and iii) same chemical potential.

Assuming a homogeneous no-slip model (Graham B. Wallis, 2020), the total pressure gradient is given by Eq. (1), composed of frictional, gravitational and accelerational components.

$$\left(\frac{dp}{dz}\right)=\left(\frac{dp}{dz}\right)_f+\left(\frac{dp}{dz}\right)_g+\left(\frac{dp}{dz}\right)_a \tag{1}$$

Under the premises of incompressible flow and uniform diameter along the tubes, the accelerational pressure gradient can be ignored.

The contribution of the frictional pressure gradient $(dp/dz)_f$ is:

$$\left(\frac{dp}{dz}\right)_f=\frac{f\rho_m U_m^2}{2D} \tag{2}$$

Where $f$ is the frictional factor, $\rho_m$ [kg/m³] is the mixture density, $U_m$ [m/s] is average fluid velocity and $D$ [m] is the tube internal diameter.

The contribution of the gravitational pressure gradient $(dp/dz)_g$ is:

$$\left(\frac{dp}{dz}\right)_g=\rho_m g\sin\theta \tag{3}$$

Where $g$ [m/s] is gravity and $\theta$ [°] is the inclination of the duct to the horizontal.

Following Guet et al. (2006), it is assumed that correlations for friction factor in single phase flow can be applied to dispersed liquid-liquid flows. Since flow regime is laminar, the friction factor $f$ is estimated as:

$$f=\frac{64}{\mathrm{Re}} \tag{4}$$

The Reynolds group for emulsions flow is:

$$\mathrm{Re}=\frac{\rho_m U_m D}{\mu_m} \tag{5}$$

Where $\rho_m$ [kg/m³] is the mixture density, $\mu_m$ [Pa.s] is the mixture viscosity, $U_m$ [m/s] is average velocity and $D$ [m] is the tube's internal diameter.

Since the information of density and viscosity is critical for the prediction of the frictional pressure gradient, some available models for determining these properties are evaluated in the results section.

## 3. RESULTS

### 3.1 Density

Figure 2 shows the density measurements as a function of temperature (from 20°C to 36°C) at pressure of 0.1 MPa measured by DSA5000M analyzer. It is observed an increase of emulsion density as increasing water volume fraction. On the other hand, density decreases with temperature.

According to Wallis (2020), the mixture density $\rho_{m,calc}$ can be expressed as a function of water density $\rho_w$, oil density $\rho_o$ and water volume fraction $C_w$, weighted by their respective concentrations as Eq. (6).

$$\rho_{m,calc}=\rho_w C_w+\rho_o(1-C_w) \tag{6}$$

Using the density data obtained from DSA5000M for both oil and water phase, the emulsion density is predicted as Eq. (6) and then compared with experimental data for emulsion density measured in the digital analyzer. Then, the error in density prediction is computed by Eq. (7) and shown in
Figure 3.

$$\Delta\rho=\frac{\rho_{m,calc}-\rho_{meas}}{\rho_{meas}} \tag{7}$$

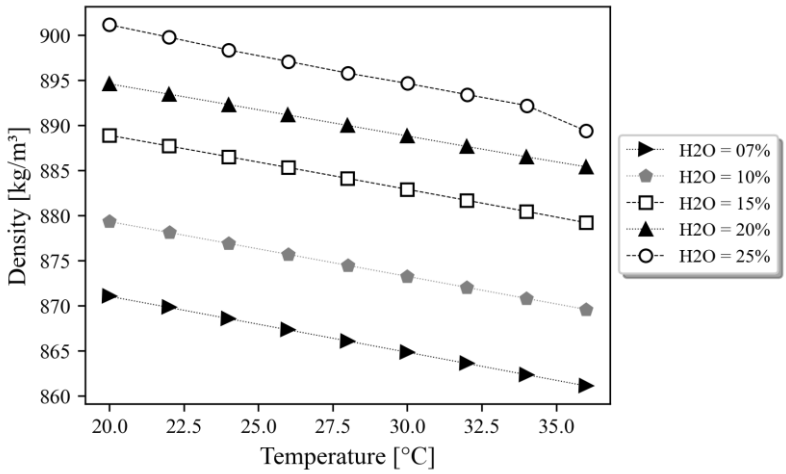


Figure 2. Experimental emulsions density

The errors in emulsion density prediction are from 0.7% to 1.4%. The prediction errors tend to remain stable for a given emulsion sample between 20°C and 36°C, with a slight increase in density prediction as temperature rises. In this case, the highest error increase occurred in the emulsion with 25% of $H_2O$ at 36°C. The prediction of density for the emulsion with 15% of $H_2O$ showed the lowest errors, while the highest errors are observed in the prediction for the emulsion with 7% of $H_2O$.

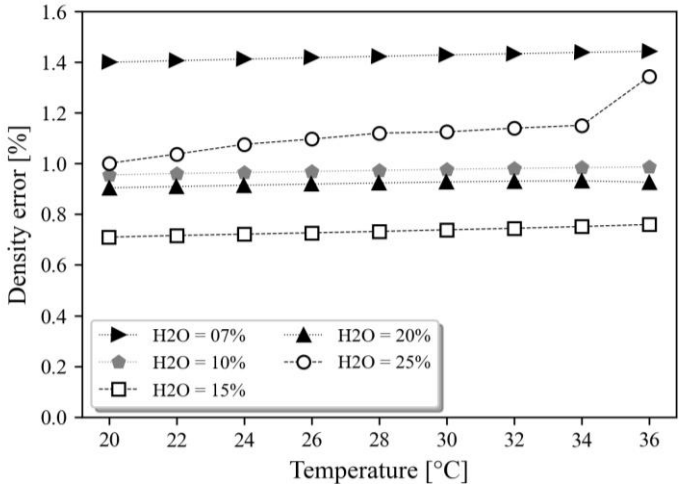


Figure 3. Error in the prediction of emulsion density

### 3.2 Rheology

Figure 4 shows the flow curves for the emulsion samples at temperatures of 25°C and 35°C, demonstrating the viscosity at shear rates in the range 100–3000 $s^{-1}$. Noticeably, the viscosities increase with the increasing of water volume fraction. The highest viscosity is reached by the emulsion sample with 25% water content, whereas the emulsion sample with 7% of $H_2O$ presents the lowest viscosity.

Results show a slightly difference in viscosity between 15% and 20% of $H_2O$. One can notice a significant increase of viscosity of the emulsion with 25% of $H_2O$, compared with the emulsion with 20% of $H_2O$. Similar behavior is obtained by Ariffina et al. (2016) for water-in-oil emulsions with crude oil.

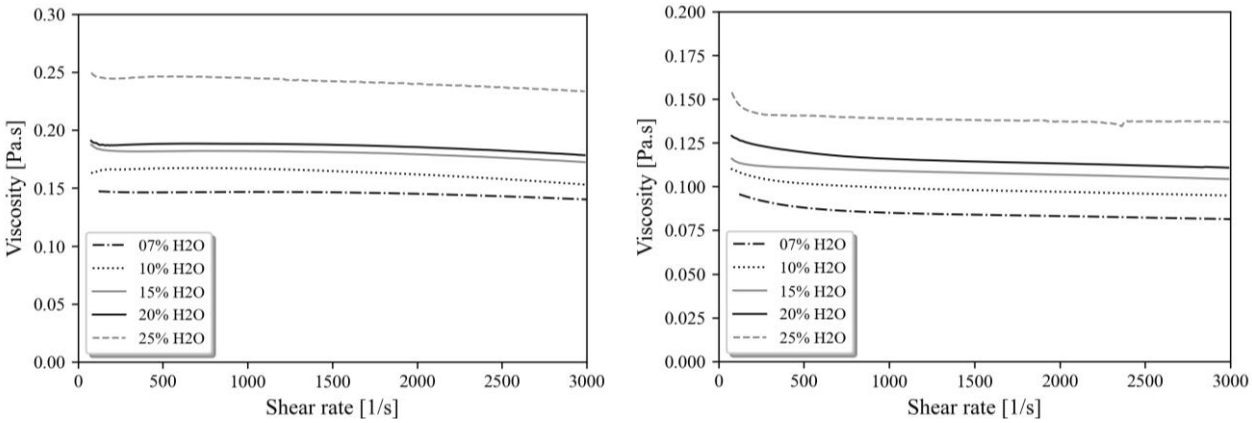


Figure 4. Flow curves of emulsion samples

Data of kinematic viscosity are shown in Table 2, including a linear regression of the viscosity as a function of temperature.

Table 2. The viscosity of emulsions

| Water fraction [%] | $\mu[Pa.s]$ at 25°C | $\mu[Pa.s]$ at 35°C | Linearization |
|---|---|---|---|
| 7 | 0.1415 | 0.0809 | $\mu = 0.2931 - 0.0060T$ |
| 10 | 0.1549 | 0.0946 | $\mu = 0.3058 - 0.0088T$ |
| 15 | 0.1741 | 0.1043 | $\mu = 0.3486 - 0.0069T$ |
| 20 | 0.1802 | 0.1103 | $\mu = 0.3549 - 0.0070T$ |
| 25 | 0.2343 | 0.1363 | $\mu = 0.4794 - 0.0098T$ |

The model for effective viscosity estimation is critical for a suitable determination of the frictional pressure gradient (Guet et al., 2006), even for dispersions such as water-in-oil emulsions. There are a number of viscosity models for liquid-liquid dispersion suggested in the literature. Some of them are presented below.

Einstein (1906) model, for small particles suspended with low dispersed phase fraction:

$$\mu_{m,1} = \mu_c(1+2.4C_w) \tag{8}$$

Taylor (1932) model for the viscosity for a fluid containing small drops of another fluid:

$$\mu_{m,2} = \mu_c\left[1+2.5C_w\left(\frac{0.4\mu_c+\mu_d}{\mu_c+\mu_d}\right)\right] \tag{9}$$

Brinkman (1952) model, which is an expansion upon Einstein's formula to accommodate moderate particle concentrations:

$$\mu_{m,3} = \mu_c(1-C_w)^{-2.5} \tag{10}$$

Thomas (1965) model, determined by extrapolation of an extensive amount of experimental data for spherical particles available at that time.

$$\mu_{m,4} = \mu_c(1+2.5C_w+10.05C_w^2+0.00273e^{16.6\,C_w}) \tag{11}$$

Elseth (2001) proposes a linear average for the effective viscosity when phase inversion point is not known.

$$\mu_{m,5} = \mu_w C_w + \mu_o(1-C_w) \tag{12}$$

Using the viscosity data for oil and water phase, the emulsions viscosity is predicted as Eqs. (8)-(12) and then compared with the experimental data of Table 2. Then, the error in density prediction is computed as follows Eq. (13).

$$\Delta\mu = \frac{\mu_{m,calc} - \mu_{meas}}{\mu_{meas}} \tag{13}$$

Results are shown in

Figure 5. A visual observation is that, for the 5 evaluated models, the behavior of the viscosity calculation error remains the same at both 25°C and 35°C.

For water fractions between 7% and 20%, the errors of the Einstein's model (1906) range from 3.1% to 8.4% at 25°C and from 5.5% to 16.3% at 35°C. For 25% of $H_2O$, the viscosity is underestimated by the Einstein's model, with errors of -9.8% at 25°C and -4.5% at 35°C. This model exhibits the best performance in predicting the emulsion viscosity with a water volume fraction between 10% and 25%.

The Taylor's model (1932) underestimated the viscosity of the emulsion, with errors ranging from -0.1% to -29.4% at 25°C and from -6.7% to -26.3% at 35°C. This model showed the highest accuracy in predicting the viscosity for the emulsion sample with 7% of water fraction.

The Brinkman's model (1955) shows errors in viscosity prediction from 10.8% to 27.9% at 25°C and from 10.1% to 26.8% at 35°C. In the model of Thomas (1965), the viscosity was overestimated, with errors from 14.9% to 44.8% at 25°C and from 15.5% to 43.5% at 35°C.

The viscosity prediction of Elseth (2001) shows a decrease in viscosity with an increase of the water volume fraction in the mixture, which underestimates the viscosity. Therefore, this model is inconsistent, with maximum errors of -57.6% at 25% water and -55.8% at 35% water.

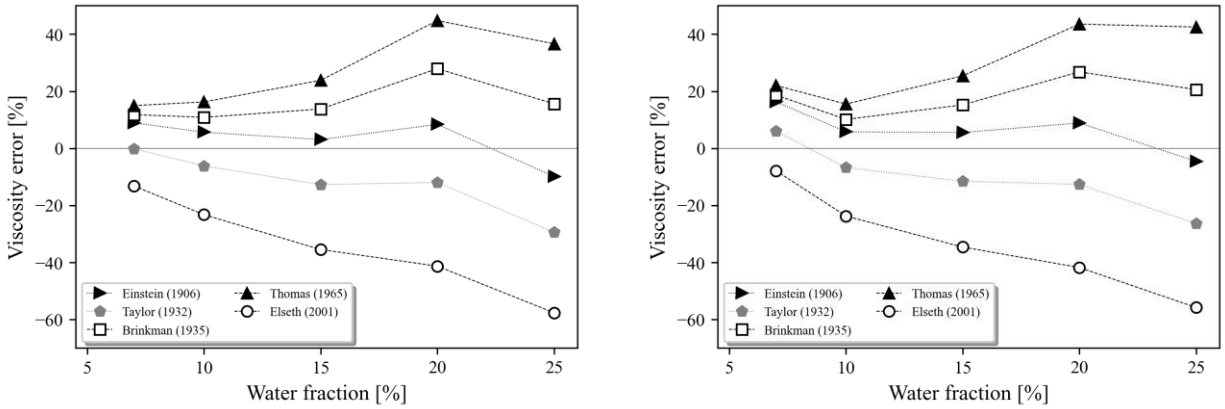


a) 25°C b) 35°C

Figure 5. Error in viscosity prediction

The results indicate that Einstein's model (1906) is the most suitable for determining the emulsion viscosity of saline water dispersed in mineral oil, for water fractions between 7% and 25%.

### 3.3 Pressure gradient

In this work, the pressure drop is evaluated by the pressure losses per meter or, in other words, by the pressure gradient $(dP/dz)$ [Pa/m]. The experimental pressure gradient is obtained using pressure readings of two-gauge pressure transmitters (PIT-2 and PIT-3 in Figure 1) and the distance $L$ between the pressure taps.

$$(dp/dz)_{\exp} = \frac{P_{PIT-2} - P_{PIT-3}}{L} \tag{14}$$

The pressure gradient can be predicted using the following flow process data: mass flow, density, viscosity and internal tube diameter.

To obtain the mean fluid velocity, first the volumetric flow rate $Q$ [m³/s] is calculated by Eq. (15), using the mass flow $\dot{m}$ [kg/s] and the density $\rho$ [kg/m³] measured by Coriolis flow meter (FIT-01).

$$Q = \frac{\dot{m}}{\rho} \tag{15}$$

Next, mean fluid velocity $U_m$ is obtained using volumetric flow rate and pipe's cross sectional area, as Eq. (16).

$$U_m = \frac{Q}{A} \tag{16}$$

Since the segment tube under study is horizontal, the term of the gravitational pressure gradient term can be neglected, and the pressure gradient is calculated according to Eq. (2) for the assumption of a homogeneous model. Density and viscosity values employed in the pressure gradient model are derived from experimental measurements. Density is interpolated from the data of

Figure 2. For the viscosity, it is used the data outlined in Table 2.

One can notice that the only parameter that is not obtained experimentally is the friction factor. Since Reynolds number range from 30 to 310, flow regime is laminar and the Hagen-Poiseuille equation is applicable for friction factor estimation, as Eq. (4).

Results are shown in

Figure 6. Each point on the graph is obtained using average data derived from an experiment under steady state conditions of mass flow (by FIT-01), density (by FIT-01), temperature (by TT-01 and TT-02), and pressure (by PT-2) at the pump discharge. Thus, it can be concluded that experiments are repeatable.

One can observe that the homogeneous model underpredicts the pressure gradient. Besides, the majority of points are between the refence lines of -10% and -25%, indicating the deviation of the models.

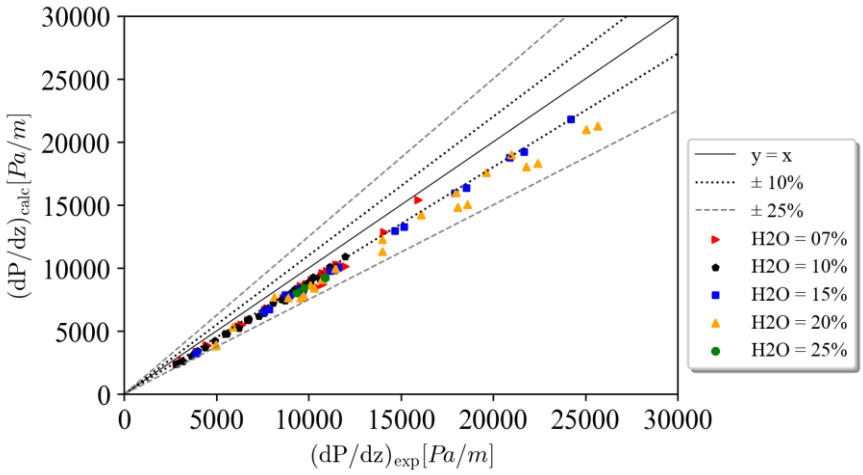


Figure 6. Pressure gradient

In order to estimate the deviations in pressure gradient prediction, Eq. (17) is used. Results are shown in Figure 7.

$$\Delta(dP/dz) = \frac{(dP/dz)_{calc} - (dP/dz)_{\exp}}{(dP/dz)_{\exp}} \tag{17}$$

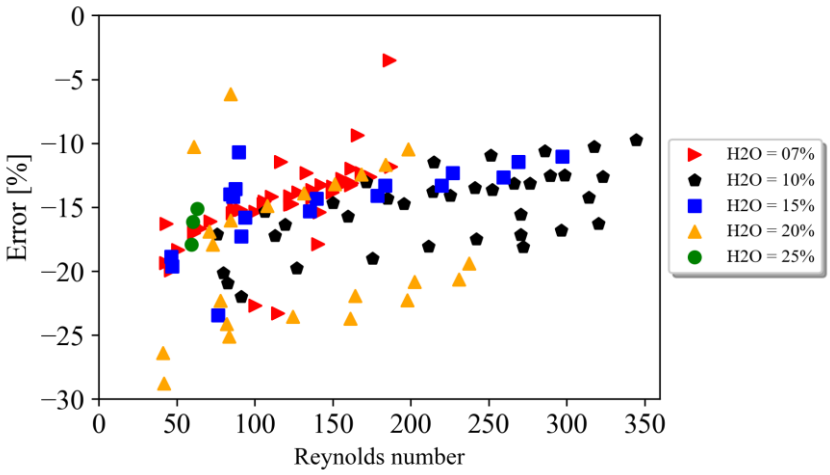


Figure 7. Error in pressure gradient prediction by homogeneous model

For the emulsion with 7% of $H_2O$, errors are between -3.5% and -23.3%. For the emulsion with 10% and 15% of $H_2O$, deviations range from -10% to -23%. For the emulsions with 20% of $H_2O$, pressure gradient errors are between -6% and -28%. Lastly, for the emulsion with 25% of $H_2O$, the deviations are between -15.1% and -17.9%. Observing Eq. (2), the only parameter which is not measured is the friction factor. Thus, the friction factor used may not be suitable for the emulsion flow.

Furthermore, it is not possible to associate the errors in pressure gradient prediction with water volume fraction of the emulsions. However, one can observe the reduction in errors with the increase of Reynolds number.

## 4. FINAL REMARKS

This study analyzed the pressure drop for water-in-oil emulsions flows, comparing models for predicting density, viscosity and pressure gradient.

The objective of this work is to analyse the pressure drop for water-in-oil emulsion flows, with viscosity ratio of 130 and water volume fraction between 7% and 25%. The evaluation is performed in a horizontal section. The density models assessment show errors from 0.7% to 1.4%. The prediction errors tend to remain stable for a given emulsion sample in the temperature range from 20°C to 36°C, with a slight increase in density errors as temperature rises. The lowest errors are found in the emulsion with 15% of $H_2O$, while the highest errors are observed in the prediction for the emulsion with 7% of $H_2O$.

In the rheology evaluation, it is found that an increase of fluid viscosity with the water volume fraction. Five models are assessed for estimation of emulsion viscosity as a function of water fraction. For the emulsion sample with 7% of $H_2O$, the best model is the one of Taylor (1932). For the other samples, with water volume fraction from 7% to 25%, the Einstein's model (1906) works best, with deviations from 3.1% to 16.3%.

The pressure gradient calculated using the homogeneous model underpredict the pressure gradient, with deviations ranging from -5% to -28%. Results indicate a trend towards error reduction as Reynolds number increases. Besides those deviations, results are repetitive, indicating that the model can be improved.

Thus, in order to improve the homogeneous model for pressure gradient prediction, it is suggested to evaluate the experimental friction factor using experimental data of the emulsion flow loop with single-phase flow with the oil phase. Then, the pressure gradient can be calculated and evaluated once mode to provide data for friction estimation.

## 5. ACKNOWLEDGEMENTS

The authors thank LabPetro/UFES and LAMEFT/UFES for giving support in fluid characterization.

The authors would like express their gratitude to Petróleo Brasileiro Company (Petrobras) and Agência Nacional do Petróleo, Gás Natural e Bio Combustíveis (ANP) by the financial support through grant 2018/00482-9.

## 6. REFERENCES

Alsabagh, A. M., Hassan, M. E., Desouky, S. E. M., Nasser, N. M., Elsharaky, E. A., & Abdelhamid, M. M. (2016). Demulsification of W/O emulsion at petroleum field and reservoir conditions using some demulsifiers based on polyethylene and propylene oxides. *Egyptian Journal of Petroleum*, *25*(4), 585–595. https://doi.org/10.1016/j.ejpe.2016.05.008

American Society for Testing and Materials. (2005). *ASTM D5002: Standard Test Method for Density and Relative Density of Crude Oils by Digital Density Analyzer*.

American Society for Testing and Materials. (2006). *ASTM D4377: Standard Test Method for Water in Crude Oils by Coulometric Karl Fischer Titration*.

American Society for Testing and Materials. (2015). *ASTM D4402: Standard Test Method for Measuring the Viscosity of Mold Powders above Their Melting Point Using a Rotational Viscometer*.

Angeli, P., & Hewitt, G. F. (1999). Pressure gradient in horizontal liquid–liquid flows. *International Journal of Multiphase Flow*, *24*(7), 1183–1203. https://doi.org/10.1016/S0301-9322(98)00006-8

Ariffin, T. S. T., Yahya, E., & Husin, H. (2016). The Rheology of Light Crude Oil and Water-In-Oil-Emulsion. *Procedia Engineering*, *148*, 1149–1155. https://doi.org/10.1016/j.proeng.2016.06.614

Brinkman, H. C. (1952). The Viscosity of Concentrated Suspensions and Solutions. *The Journal of Chemical Physics*, *20*(4), 571–571. https://doi.org/10.1063/1.1700493

Corona, R. R. B., Sad, C. M. S., da Silva, M., de Castro, E. V. R., Quintela, E. F., & Ramos, R. (2023). Selecting a model fluid with properties similar to crude oil to test the formation of W/O emulsions. *Journal of Petroleum Science and Engineering*, *221*. https://doi.org/10.1016/j.petrol.2022.111265

Einstein, A. (1906). Eine neue Bestimmung der Moleküldimensionen. *Annalen Der Physik*, *324*(2), 289–306. https://doi.org/10.1002/andp.19063240204

Elseth, G. (2001). *An Experimental Study of Oil / Water Flow in Horizontal Pipes*. The Norwegian University of Science and Technology.

Graham B. Wallis. (2020). *One-dimensional Two-phase Flow*. Courier Dover Publications.

Guet, S., Rodriguez, O. M. H., Oliemans, R. V. A., & Brauner, N. (2006). An inverse dispersed multiphase flow model for liquid production rate determination. *International Journal of Multiphase Flow*, *32*(5), 553–567. https://doi.org/10.1016/j.ijmultiphaseflow.2006.01.008

Kempin Júnior, E., Roberti, J. T. A., Franco, L. G., & Ramos, R. (2022). Engineering aspects on flow similarity for design water-in-oil emulsion circuit. In *Multiphase Flow Dynamics* (1st ed., Vol. 1, pp. 255–265). Springer.

Rodriguez, O. M. H., & Oliemans, R. V. A. (2006). Experimental study on oil–water flow in horizontal and slightly inclined pipes. *International Journal of Multiphase Flow*, *32*(3), 323–343. https://doi.org/10.1016/j.ijmultiphaseflow.2005.11.001

Sullivan, A. P., Zaki, N. N., Sjöblom, J., & Kilpatrick, P. K. (2008). The Stability of Water-in-Crude and Model Oil Emulsions. *The Canadian Journal of Chemical Engineering*, *85*(6), 793–807. https://doi.org/10.1002/cjce.5450850601

Taylor, G. I. (1932). The viscosity of a fluid containing small drops of another fluid. *Proceedings of the Royal Society of London. Series A, Containing Papers of a Mathematical and Physical Character*, *138*(834), 41–48. https://doi.org/10.1098/rspa.1932.0169

Thomas, D. G. (1965). Transport characteristics of suspension: VIII. A note on the viscosity of Newtonian suspensions of uniform spherical particles. *Journal of Colloid Science*, *20*(3), 267–277. https://doi.org/10.1016/0095-8522(65)90016-4

van der Zande, M. J. (1998). Break-up of oil droplets in the production system. *Proceedings of ASME Energy Sources Technology Conference and Exhibition*.

## 7. RESPONSIBILITY NOTICE

The author(s) is (are) the only responsible for the printed material included in this paper.